

Article

# Cocrystallization of Progesterone with Nitrogen Heterocyclic Compounds: Synthesis, Characterization, Calculation and Property Evaluation

Juan Xu <sup>1,†</sup>, Wei Gao <sup>2,†</sup>, Qi Zhang <sup>3,\*</sup> and Lifeng Ning <sup>1,\*</sup>

<sup>1</sup> NHC Key Laboratory of Reproductive Health Engineering Technology Research, National Research Institute for Family Planning, Beijing 100081, China; xujuan@nrifp.org.cn

<sup>2</sup> School of Pharmacy, Guangdong Pharmaceutical University, Guangzhou 510006, China; gaowei@gdpu.edu.cn

<sup>3</sup> School of Chemistry and Chemical Engineering, Beijing Institute of Technology, Beijing 100081, China

\* Correspondence: zhangqi@bit.edu.cn (Q.Z.); ninglifeng@nrifp.org.cn (L.N.); Tel.: +86-010-62179135 (L.N.)

† These authors contributed equally to this work.

**Abstract:** Progesterone injection is oily because of its poor solubility. It is necessary to develop new dosage forms or delivery methods for Progesterone. Six cocrystals of Progesterone with nitrogen heterocyclic compounds (2,6-diaminopyridine, isonicotinamide, 4-aminopyridine, aminopyrazine, picolinamide and pyrazinamide) have been designed and prepared by ethyl acetate-assisted grinding, of which four cocrystals (2,6-diaminopyridine, isonicotinamide, 4-aminopyridine and aminopyrazine) had single crystal data in 1:1 stoichiometry. Metadynamics-genetic crossing was used to search and optimize various cluster structures to explain the reason the other two cocrystals could not be obtained with suitable size for single crystal X-ray diffraction. In contrast to the carboxyl group, the amide group and amino group were good substituents in the pyridine/pyrazine ring for cocrystallization with Progesterone, which meant inductive effect played an important role in nitrogen heterocyclic compounds containing reactive hydrogen. All cocrystals were more soluble than Progesterone in water, and Progesterone–pyrazinamide cocrystal featured the best water solubility performance with an approximately six-fold increase over free Progesterone. This successful attempt provides an effective route for designing and manufacturing novel solid states of Progesterone.

**Keywords:** progesterone; pharmaceutical cocrystals; nitrogen heterocyclic compounds; cocrystal particles with suitable size; metadynamics-genetic crossing



**Citation:** Xu, J.; Gao, W.; Zhang, Q.; Ning, L. Cocrystallization of Progesterone with Nitrogen Heterocyclic Compounds: Synthesis, Characterization, Calculation and Property Evaluation. *Molecules* **2023**, *28*, 4242. <https://doi.org/10.3390/molecules28104242>

Academic Editor: Graham Saunders

Received: 13 April 2023

Revised: 12 May 2023

Accepted: 15 May 2023

Published: 22 May 2023



**Copyright:** © 2023 by the authors. Licensee MDPI, Basel, Switzerland. This article is an open access article distributed under the terms and conditions of the Creative Commons Attribution (CC BY) license (<https://creativecommons.org/licenses/by/4.0/>).

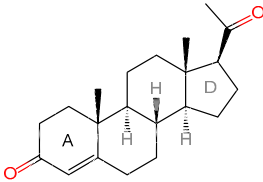
## 1. Introduction

Progesterone (PRO, Table 1) is the main bioactive progestational hormone secreted by the ovary [1]. PRO can not only induce the transition of the endometrium to the secretory stage and increase endometrium receptance to facilitate the implantation of a fertilized egg but also act on the uterus, providing a good internal environment for the maintenance of pregnancy [2,3]. PRO injection is oily because of its poor solubility [4,5]. The advantages of oily injection are the exact curative effect and low price, while the disadvantages are injection site pain, stimulation and scleroma. Due to the first-pass effect of the liver, the absolute bioavailability of oral PRO is only 6~8% [6,7]. It is necessary to develop new dosage forms or delivery methods of PRO.

A pharmaceutical cocrystal is a binary or multi-component crystal system formed by the combination of drug active ingredient (API) and cocrystal former (CCF) through hydrogen bonds or other weak interactions between molecules [8–10]. By selecting CCFs with different properties, the physicochemical properties of API can be improved or designed at the molecular level without changing its structure, which is very important to maintain the biological activity of API in vivo [11–14]. PRO is a good substrate for cocrystallization

because there are two carbonyl groups in the molecule that can act as hydrogen bond acceptors, and the steroidal parent nucleus can produce conjugation effects [15–18].

**Table 1.** Brief introduction to Progesterone.

Parameters	Data
Chemical name	4-Pregnene-3,20-dione
Chemical formula	$C_{21}H_{30}O_2$
Molecular weight	$314.46 \text{ g}\cdot\text{mol}^{-1}$
CAS Registry No.	57-83-0
Chemical structure	

With our consistent aim to further explore the solid-state forms of PRO, cocrystals of PRO with 2,6-diaminopyridine (DMP), isonicotinamide (INA), 4-aminopyridine (AP), aminopyrazine (APZ), picolinamide (PA) and pyrazinamide (PZA) were prepared and evaluated in stability and water solubility (Figure 1). Four cocrystals (DMP, INA, AP, APZ) had single crystal data in 1:1 stoichiometry. Meanwhile, two cocrystals (PA, PZA) had no suitable size for single-crystal X-ray diffraction. The reasons were calculated by MTD-GC (metadynamics-genetic crossing). The calculation results showed that the tetramers (2PRO/2PA) were stable, and the structural fluctuations of the tetramers cluster in ethyl acetate solvent were increased and led to a deficiency in order structure. In contrast to the carboxyl group, the amide group and amino group were good substituents in the pyridine/pyrazine ring. This meant that for the cocrystallization of nitrogen heterocyclic compounds containing reactive hydrogen, the inductive effect played an important role. The cocrystals have been characterized by nuclear magnetic resonance, infrared spectroscopy, thermogravimetric analysis, differential scanning calorimetry, scanning electron microscopy, powder X-ray diffraction and single crystal X-ray diffraction (for PRO-DMP, INA, AP, APZ). The stability and solubility have also been explored systematically.

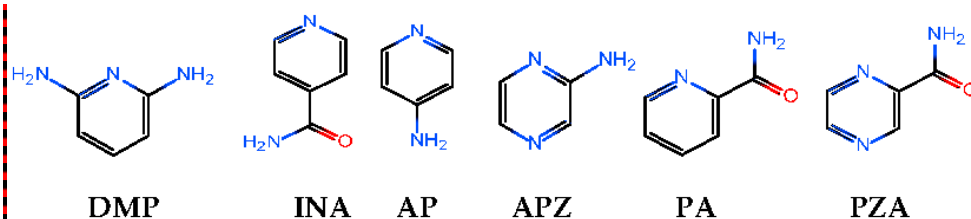


**Figure 1.** Chemical structures of the CCFs used in this study.

## 2. Results

### 2.1. General Analysis

The PXRD patterns of six cocrystals showed that the diffraction peaks had obvious differences in the position, number, strength, geometric topology and so on (Figure 2). SEM images showed that each cocrystal had unique crystal habits and morphological characteristics. PRO had block morphology, PRO-DMP and PRO-PA had smaller flake morphology, PRO-INA had bigger flake morphology, PRO-APZ, PRO-AP and PRO-PZA had irregular morphology (Figure S1). In FT-IR spectra (Figure S2), the asymmetric stretching vibrations at  $3500\text{--}3100 \text{ cm}^{-1}$  indicated the presence of the amino or amide groups in all six cocrystals. The  $^1\text{H-NMR}$  spectra clearly showed the 1:1 stoichiometry of PRO to the CCFs in all six cocrystal forms (Figure S3). The chemical shift of PRO in  $^1\text{H-NMR}$  was between 0.67 and 5.63 ppm, and nitrogen heterocyclic compounds had a larger chemical

shift between 5.63 and 9.18 ppm. A sharp endothermic peak at 132 °C was shown in the TGA-DSC curve of PRO, corresponding to the melting point of PRO. Six cocrystals had similar thermodynamic behaviors with weight loss (Figure S4). The melting points of PRO and six cocrystals are shown in Table 2.

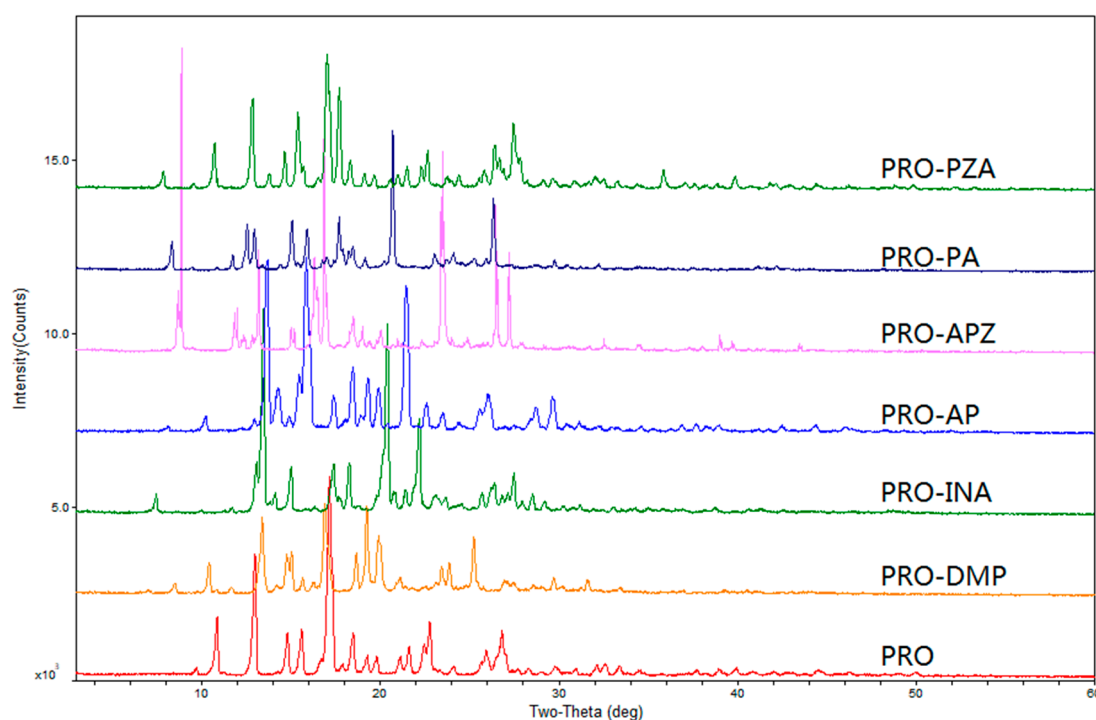


**Figure 2.** Powder X-ray diffraction (PXRD) of PRO and 6 cocrystals.

**Table 2.** Melting points PRO and 6 cocrystals.

Compounds	Melting Points (°C)
PRO	132
PRO-DMP	110
PRO-INA	130
PRO-APZ	112
PRO-AP	122
PRO-PA	122
PRO-PZA	126

## 2.2. Single X-ray Diffraction Experiments

The crystallographic parameters of PRO-DMP/INA/AP/APZ are listed in Table 3. The single X-ray diffraction pattern is shown in Figure 3. PRO-DMP/INA/AP/APZ cocrystals were composed of PRO and CCF with a ratio of 1:1.

**Table 3.** Crystallographic parameters of PRO-DMP, INA, AP, APZ.

Compounds	PRO-DMP	PRO-INA	PRO-AP	PRO-APZ
CCDC no.	2,131,361	2,131,362	2,131,375	2,131,374
Empirical formula	C <sub>26</sub> H <sub>37</sub> N <sub>3</sub> O <sub>2</sub>	C <sub>27</sub> H <sub>36</sub> N <sub>2</sub> O <sub>3</sub>	C <sub>26</sub> H <sub>36</sub> N <sub>2</sub> O <sub>2</sub>	C <sub>25</sub> H <sub>35</sub> N <sub>3</sub> O <sub>2</sub>
Formula weight	423.59	436.58	408.57	409.56
Temperature / K	116.10 (14)	116.40 (14)	113.10 (14)	113.35 (10)
Crystal system	monoclinic	orthorhombic	orthorhombic	triclinic
Space group	P2 <sub>1</sub>	P2 <sub>1</sub> 2 <sub>1</sub> 2 <sub>1</sub>	P2 <sub>1</sub> 2 <sub>1</sub> 2 <sub>1</sub>	P <sub>1</sub>

Table 3. Cont.

Compounds	PRO-DMP	PRO-INA	PRO-AP	PRO-APZ
a / Å	13.0819 (5)	7.8943 (5)	7.6234 (6)	10.4819 (10)
b / Å	18.6192 (6)	12.9909 (17)	12.2741 (8)	10.7971 (10)
c / Å	19.7511 (8)	46.685 (2)	24.4042 (16)	11.1480 (11)
$\alpha$ / °	90.00	90.00	90.00	113.753 (9)
$\beta$ / °	107.375 (4)	90.00	90.00	99.185 (8)
$\gamma$ / °	90.00	90.00	90.00	90.928 (8)
Volume / Å <sup>3</sup>	4591.3 (3)	4787.7 (7)	2283.5 (3)	1135.45 (19)
Z	8	8	4	2
$\rho_{\text{calc}}$ / mg mm <sup>-3</sup>	1.226	1.211	1.188	1.198
$\mu$ / mm <sup>-1</sup>	0.078	0.078	0.075	0.076
F (000)	1840	1888	888	444
Crystal size / mm <sup>3</sup>	0.40 × 0.35 × 0.33	0.40 × 0.40 × 0.31	0.22 × 0.21 × 0.21	0.45 × 0.43 × 0.42

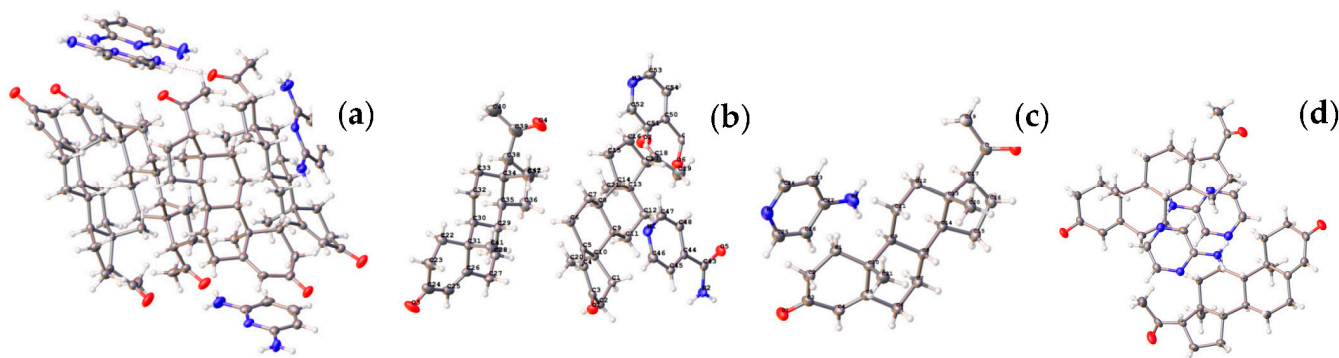


Figure 3. Structure of (a) PRO-DMP, (b) PRO-INA, (c) PRO-AP and (d) PRO-APZ.

### 2.3. Stability Analysis

Stability experiment was performed to investigate the physical stability and transformation of the sample under different storage environments and physiological conditions. PRO and six cocrystals all showed excellent physical stability in high temperature, high humidity, high light intensity condition and in water suspension conditions (Figure S5).

### 2.4. In Vitro Dissolution Tests

In preparing new alternative crystal forms of chemical entities, water solubility was one of the most important physicochemical parameters. In addition, solubility was closely related to the bioavailability of drugs in vivo. Since PRO has poor solubility in water (0.41 mg·mL<sup>-1</sup>), the synthesis of cocrystals is attractive. PRO-DMP/INA/AP/APZ/PA featured 1.22 mg·mL<sup>-1</sup>, 1.74 mg·mL<sup>-1</sup>, 1.81 mg·mL<sup>-1</sup>, 1.55 mg·mL<sup>-1</sup> and 1.63 mg·mL<sup>-1</sup>, respectively, being 3- to 4.5-fold equilibrium concentration in water when compared with PRO used in the solubility experiments (Figure 4). In particular, for PRO-PZA, the equilibrium concentration reached 2.65 mg·mL<sup>-1</sup>, which was approximately 6.5-fold as large as the solubility of free PRO. This result suggested that PRO-PZA could be a suitable candidate for novel PRO pharmaceutical formulations with improved solubility. Beyond that, there was no significant difference in PXRD patterns between raw material and the residual phases after the solubility experiments for PRO and all cocrystals (Figure S5).

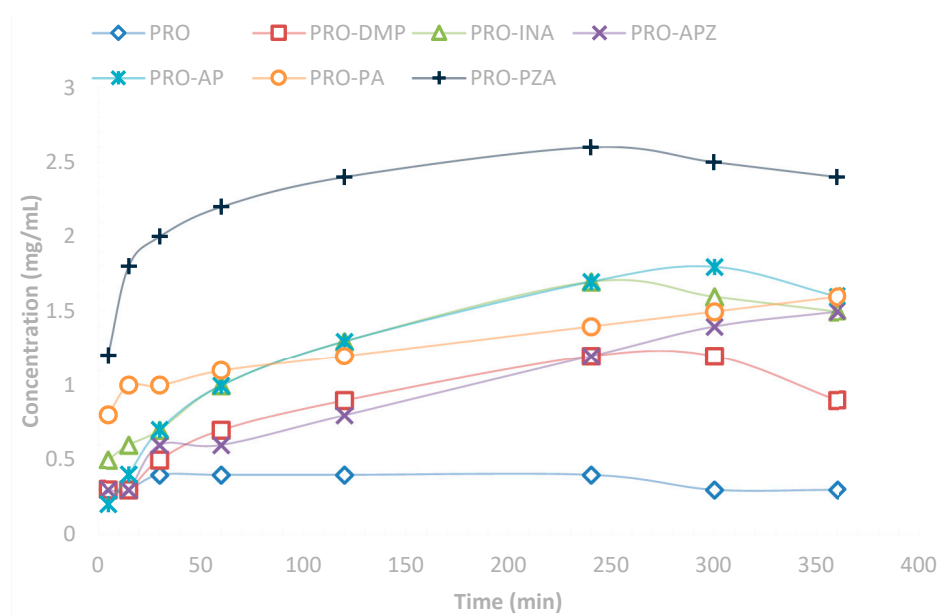


**Figure 4.** In vitro dissolution profiles for commercial PRO and 6 cocrystals in water.

### 2.5. Nitrogen Heterocyclic Ring CCFs That Cannot Form Cocrystals with PRO

Under ethyl acetate-assisted grinding conditions, some nitrogen heterocyclic ring CCFs could not form cocrystals with PRO, such as heterocyclic amino acid and purine/pyrimidine (Table 4). There were probably two reasons. One was the hydrogen bound to the CCF too tightly; the other was the CCFs themselves being prone to forming intramolecular/intermolecular hydrogen bonds. As a result, they failed to form cocrystals with PRO.

**Table 4.** Some nitrogen heterocyclic ring CCFs could not form cocrystals with PRO.

Category	Specific Compounds
Heterocyclic amino acid	L-histidine, L-proline, DL-tryptophan
Purine/pyrimidine	adenine, cytosine, guanine, thymine, uracil
Heterocyclic compound	2-acetylthiazole, 2,3'-bipyridine, 4,4'-bipyridine, folic acid, 5-(2-hydroxyethyl)-4-methylthiazole, imidazole, orotic acid, piperazine, pyrazine, pyridine, saccharin

### 2.6. Substituted Pyridine Derivatives

Pyridine could not form cocrystal with PRO. As shown in Tables 5 and 6, in contrast to the carboxyl group, amide group and amino group were good substituents, which meant the electron inductive effect showed a very strong effect in cocrystallization of PRO and pyrazine derivatives. Single crystal data could be obtained when there was a p-NH<sub>2</sub> or p-CONH<sub>2</sub> on pyridine ring. The cocrystal of o-CONH<sub>2</sub> on pyridine ring (PA) with PRO could be confirmed by PXRD, TG, DSC and <sup>1</sup>H-NMR, while the single crystal could not be obtained successfully.

**Table 5.** Cocrystallization between PRO and pyridine with one substituent.

Pyridine with One Substituent	<i>o</i>	<i>m</i>	<i>p</i>
-COOH	–	–	–
-CONH <sub>2</sub>	+ (PA)	–	+ √ (INA)
-NH <sub>2</sub>	–	–	+ √ (AP)

+: positive cocrystallization; –: negative cocrystallization; √: single crystal.

**Table 6.** Cocrystallization between PRO and pyridine with two substituents.

Pyridine with Two Substituents	Position	Reaction
-COOH	2.6	–
-NH <sub>2</sub>	2.6	+ √ (DMP)

+: positive cocrystallization; –: negative cocrystallization; √: single crystal.

### 2.7. Substituted Pyrazine Derivatives

Pyrazine could not form cocrystal with PRO. Similar to pyridine derivatives, the cocrystallization could not proceed between PRO and piperazinecarboxylic acid. The reaction could take place between PRO and piperazine with amide or amino-substituted (Table 7). The results of PRO-PZA were similar to PRO-PA, cocrystallization took place, but the single crystal was difficult to obtain. Cocrystallization of PRO and piperazine with methyl-substituted was negative because there was no active hydrogen in the molecule.

**Table 7.** Cocrystallization between PRO and substituted pyrazine.

Substituted Pyrazine	Reaction
-COOH	–
-CONH <sub>2</sub>	+ (PZA)
-NH <sub>2</sub>	+ √ (APZ)
-CH <sub>3</sub>	–
-CH <sub>3</sub> , -CH <sub>3</sub> , -CH <sub>3</sub>	–
-CH <sub>3</sub> , -CH <sub>3</sub> , -CH <sub>3</sub> , -CH <sub>3</sub>	–

+: positive cocrystallization; –: negative cocrystallization; √: single crystal.

## 3. Discussion

The crystal formation of PRO cocrystals included two processes: nucleation and growth. In the nucleation stage, the clusters generated by weak interactions between API and CCF generally retained the essential structural characteristics of cocrystals. The cocrystal molecules were in an ordered arrangement with the assistance of electron-donating groups to precipitate crystals with suitable sizes for single-crystal testing. However, the electron-withdrawing group was unable to arrange the cocrystal molecules in order, or the intermolecular force between cocrystal molecules was too weak to form appropriate unit cells, resulting in the precipitation of thin/small/hardened cocrystal particles, which were unsuitable for SXR. The reason for not obtaining a single crystal was explained by calculation. The initial structure was constructed according to the electrostatic potential and synthetic subrules for cocrystal formation of PRO and PA. MTD-GC (metadynamics-genetic crossing) was used to search and optimize various cluster structures, followed by sorting their stability with the GFN0-xTB method [19]. The solvent effect of ethyl acetate was calculated by the GBSA model. The above work was performed in the CREST [20] and xTB software [21].

In general, dimers (1API/1CCF) were stable for the cocrystal, which could obtain single-crystal data. The calculation results showed that the tetramers (2PRO/2PA) were stable, with a stable hexagonal cyclic hydrogen bond formed between the amide groups of two adjacent PA. Two molecules of PRO were stabilized with adjacent PA through the Van der Waals force (Figure 5). The thin lines reflected the various cluster structure and the thick lines were the most stable. Figure 6 shows the tetramer structure in ethyl acetate as the solvent crystallized experimentally. The structural fluctuations of the cluster in ethyl acetate solvent were increased and led to a deficiency in order structure, which might be one of the reasons why the PRO-PA crystal was difficult to grow in ethyl acetate. Dissimilarly, the CIF file of PRO-INA showed that one molecule of PRO was hydrogen-bonded to two molecules of INA, and there was no interaction between adjacent PRO molecules (Figure 7).

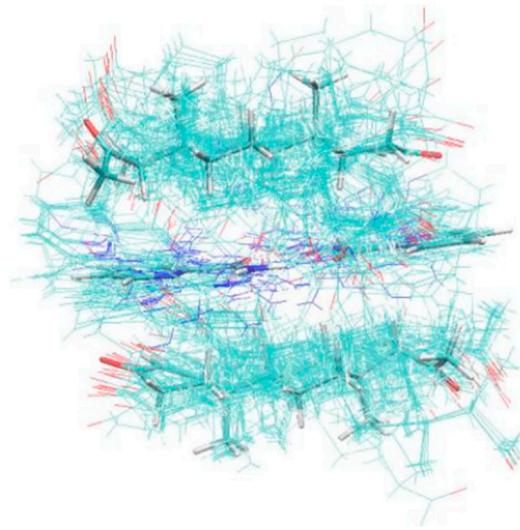


**Figure 5.** Polymer diagram of 2PRO-2PA.

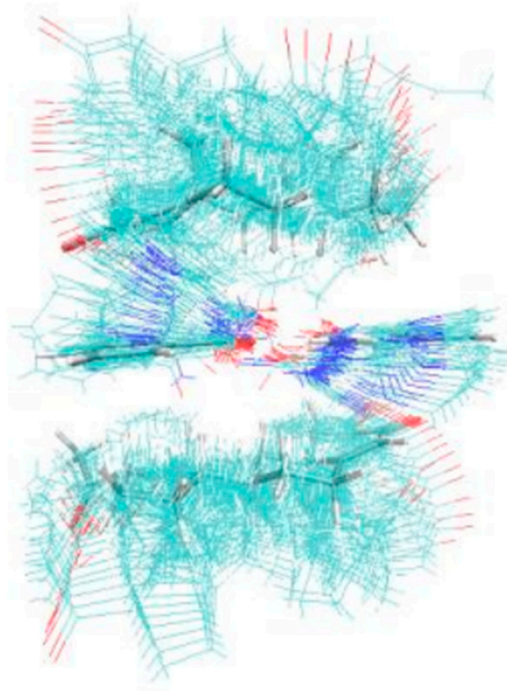


**Figure 6.** Polymer diagram of 2PRO-2PA in ethyl acetate.

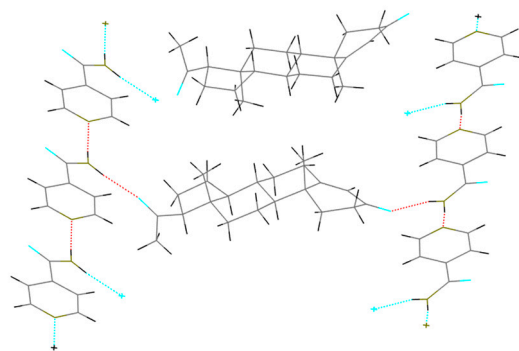


**Figure 7.** Polymer diagram of CIF file for PRO-INA.

## 4. Materials and Methods

### 4.1. Materials

PRO (purity 99.4%) was obtained from Zhejiang Xianju Pharmaceutical Co., Ltd. (Xianju, China, Lot number: Y011-200507). CCFs were purchased from Shanghai Bide Pharmatech Co., Ltd. (Shanghai, China). All reagents and chemicals were commercially available and used directly.

### 4.2. Preparation of the Cocrystals and Single Crystals

All PRO cocrystals were prepared by ethyl acetate-assisted grinding in a ball mill (QM3SP2L, Nanjing Chishun Science & Technology Co., Ltd., Nanjing, China). The grinding experiments were performed by the addition of an equimolar of PRO (943.4 mg, 3 mmol), corresponding CCFs (3 mmol) and 0.1 mL ethyl acetate to a 250 mL agate grinding jar. The mixture was then ground at a frequency of 28 Hz for 40 min [22].

An appropriate amount of the PRO cocrystals was dissolved in ethyl acetate. The solvent was slowly volatilized, and the obtained crystals were analyzed by single-crystal X-ray diffraction.

### 4.3. General Methods

Powder X-ray diffraction (PXRD) patterns were recorded with a BRUKER D8 advance diffractometer system with CuK $\alpha$ 1 radiation ( $\lambda = 1.5406 \text{ \AA}$ , 40 kV, 40 mA) over the interval  $3\text{--}60^\circ/2\theta$ . Thermo gravimetric analysis-differential scanning calorimetry (TG-DSC) was conducted on TGA/DSC<sup>3+</sup> equipment under a flow of nitrogen (20 mL/min) at a scan rate of  $10^\circ\text{C}/\text{min}$  from 40 to  $400^\circ\text{C}$ . Fourier transform infrared spectroscopy (FT-IR) was performed with a Bruker EQUINOX 55 FT-IR spectrometer (Billerica, MA, USA). A total of 64 scans were collected over a range of  $4000\text{--}400 \text{ cm}^{-1}$  with a resolution of  $0.2 \text{ cm}^{-1}$  for each sample. A Jeol JSM-6100 scanning electron microscope (SEM, Akishima, Japan) was used to obtain photomicrographs. Samples were mounted on a metal stub with adhesive tape and coated under a vacuum with platinum. Nuclear magnetic resonance ( $^1\text{H-NMR}$ ) was recorded using a Bruker 400 MHz instrument using DMSO- $d_6$  as a solvent and TMS as an internal standard. Single crystal X-ray diffraction (SXRD) data were collected by Rigaku AFC-10/Saturn 724-CCD diffractometer (Tokyo, Japan) equipped with a graphite-monochromatized MoK $\alpha$  radiation ( $0.71073 \text{ \AA}$ ) up to a 2 h limit of  $50.0^\circ$  at room temperature ( $25^\circ\text{C}$ ).

### 4.4. Stability Study

For the stability study, the powder samples of 100–200 mg cocrystals in 5 mL uncapped glass vials were placed in a stability chamber (Bluepard Yiheng, Shanghai, China) at  $60 \pm 2^\circ\text{C}$ ,  $90 \pm 5\%$  RH and light exposure of  $4500 \pm 500 \text{ lx}$  for 10 days, respectively. Then, the samples were analyzed by PXRD for 5 and 10 days.

### 4.5. In Vitro Dissolution Tests

The in vitro dissolution tests was carried out according to the guideline and procedure specified in Chinese Pharmacopeia. The dissolution of the experiment was performed on the dissolution apparatus (RC806D, Tiandatianfa, Tianjin, China) at  $37^\circ\text{C}$  with the rotation speed set at 100 rpm, and the samples were taken at 5, 15, 30, 60, 120, 240, 300 and 360 min. The samples were filtered through  $0.45 \mu\text{m}$  membrane filters and measured on HPLC (LC-20A, Japanese Shimadzu Corporation, Kyoto, Japan) coupled with a diode array detector. The wavelength was 254 nm, and the chromatographic column was Inertsil ODS-3 C18 ( $5 \mu\text{m} \times 4.6 \text{ mm} \times 150 \text{ mm}$ ). The mobile phase was methanol/water (65:35, *v:v*). The flow rate of the mobile phase was  $1 \text{ mL}/\text{min}$ , and the injection volume was  $20 \mu\text{L}$ .

## 5. Conclusions and Outlook

In the present work, six PRO cocrystals were prepared and evaluated in stability and solubility, of which four cocrystals had single crystal data. All cocrystals were prepared by

grinding in a ball mill without solvent. They were more soluble than PRO. The exploration of more CCFs is still underway.

Based on the cases studied in this paper, the empirical rules of PRO-CCFs were summarized according to the electronic effects of the aromatic substituent. Such rules could be used to rationalize the possibility of a combination of PRO with various CCFs, but there was no guarantee of working in other cases. The specific CCF of formed or failed cocrystals is a very complex process driven by many factors. At present, choosing CCFs relies largely on experience. Meanwhile, several strategies and methods have been developed to aid in predicting the possibility of CCF cocrystal formation.

Among these approaches, data-driven machine learning (ML) methods can provide robust mathematical models to predict the CCFs selection, improved by good quality and amount of data from statistical perspectives. In this work, a reliable cocrystal dataset for PRO-CCFs was obtained by collecting successful and failed samples. The failed cases were particularly useful, which was not readily available to be found in published papers.

Benefiting from our rich data and experimental practices, we are building ML-based classifiers to predict PRO-CCFs cocrystal formation. Selected molecular descriptors can be acted as “input” while a successful cocrystal or not as “output”. The former involves molecular size, flexibility, Hansen solubility parameters, hydrogen bond tendency, etc. The predicted models will be trained by random forest (RF), support vector machine (SVM) and artificial neural network (ANN) algorithms. We expect such models to become useful tools for the design of cocrystal.

**Supplementary Materials:** The following supporting information can be downloaded at: <https://www.mdpi.com/article/10.3390/molecules28104242/s1>, Figure S1: Scanning electron microscope (SEM) of PRO and 6 cocrystals (10 $\mu$ m); Figure S2: Fourier transform infrared spectroscopy (FT-IR) of PRO and 6 cocrystals; Figure S3:  $^1\text{H}$  nuclear magnetic resonance spectra ( $^1\text{H-NMR}$ ) of PRO and 6 cocrystals; Figure S4: Thermal analysis of PRO and 6 cocrystals; Figure S5: The stability experiment of PRO and 6 cocrystals under different conditions.

**Author Contributions:** Investigation, writing—original draft, data curation, J.X.; calculation, except quantum chemical calculations, W.G.; quantum chemical calculations, Q.Z.; project administration, writing—review and editing, L.N. All authors have read and agreed to the published version of the manuscript.

**Funding:** This research was funded by the Non-profit Central Research Institute Fund of the National Research Institute For Family Planning, grant number 2022GJZ06; Innovation and Strengthening project of Guangdong Pharmaceutical University-Special project of Guangdong Education Commission, grant number 2020KZDZX1128 and Research projects of the Chinese Medicine Council of Guangdong Province, grant number 20231209.

**Data Availability Statement:** The data presented in this study are available in Supplementary Materials.

**Conflicts of Interest:** The authors declare no conflict of interest.

**Sample Availability:** Samples of the six cocrystals are available from the authors.

## References

1. Witcher, A.; Comley, K.; Cottrell, J.; Counningham, M., Jr.; Ibrahim, T.; LaMarca, B.; Amaral, L.M. Progesterone induced blocking factor inhibition causes inflammation and endothelial dysfunction in pregnant Sprague Dawley rats. *Am. J. Obstet. Gynecol.* **2020**, *222*, S5–S6. [[CrossRef](#)]
2. Soltanyzadeh, M.; Salimi, A.; Halabian, R.; Ghollasi, M. The effect of female sex steroid hormones on osteogenic differentiation of endometrial stem cells. *Mol. Biol. Rep.* **2020**, *47*, 3663–3674. [[CrossRef](#)] [[PubMed](#)]
3. Burns, G.W.; Brooks, K.E.; O’Neil, E.V.; Hagen, D.E.; Behura, S.K.; Spencer, T.E. Progesterone effects on extracellular vesicles in the sheep uterus. *Biol. Reprod.* **2018**, *98*, 612–622. [[CrossRef](#)] [[PubMed](#)]
4. Tisdale, J.E.; Jaynes, H.A.; Overholser, B.R.; Sowinski, K.M.; Flockhart, D.A.; Kovacs, R.J. Influence of oral Progesterone administration on drug-induced QT interval lengthening: A randomized, double-blind, placebo-controlled crossover study. *JACC-Clin. Electrophys.* **2016**, *2*, 765–774. [[CrossRef](#)] [[PubMed](#)]

5. Kataoka, Y.; Wada, M.; Bito, M.; Asai, J.; Katoh, N. Subcutaneous nodules at Progesterone injection sites after fertility treatment. *Australas. J. Dermatol.* **2018**, *60*, 143–144. [[CrossRef](#)]
6. Davey, D.A. Menopausal hormone therapy: A better and safer future. *Climacteric* **2018**, *21*, 454–461. [[CrossRef](#)]
7. Joseph, A.A.; Hill, J.L.; Patel, J.; Patel, S.; Kincl, F.A. Sustained-release hormonal preparations XV: Release of Progesterone from cholesterol pellets in vivo. *J. Pharm. Sci.* **2010**, *66*, 490–493. [[CrossRef](#)]
8. Rodgers, J.E. Sacubitril/Valsartan: The newest addition to the toolbox for guideline-directed medical therapy of heart failure. *Am. J. Med.* **2017**, *130*, 635–639. [[CrossRef](#)]
9. Gong, X.F.; Xu, J.; Ning, L.F.; Li, P.; Chen, X.F.; Wang, H.P. The co-crystal structure of (17b)-estra-1,3,5(10)-triene-3, 17diol-Acetamid(1/1), C<sub>20</sub>H<sub>29</sub>NO<sub>3</sub>. *Z. Krist.-New Cryst. St.* **2020**, *235*, 31–34. [[CrossRef](#)]
10. Chen, X.F.; Xu, J.; Li, P.; Wang, H.P.; Ning, L.F. 6-methyl-3,20-dioxo-19-norpregna-4,6-dien-17-ylacetate-2,4-dihydroxy-benzoic acid (1/1), C<sub>30</sub>H<sub>36</sub>O<sub>8</sub>. *Z. Krist.-New Cryst. St.* **2020**, *235*, 453–455. [[CrossRef](#)]
11. Aakeröy, C.B.; Salmon, D.J. Building cocrystals with molecular sense and supramolecular sensibility. *Cryst. Eng. Comm.* **2005**, *7*, 439–448. [[CrossRef](#)]
12. Du, R.K.; Xu, J.; Zhang, L.; Ning, L.F.; Li, S. Ethinyl estradiol cocrystals assembled by chains structures: Improvement in stability and solubility. *New J. Chem.* **2019**, *43*, 16889–16897. [[CrossRef](#)]
13. Xu, J.; Du, R.K.; Wu, L.Y.; Zhang, X.R.; Guan, S.; Zhang, L.; Ning, L.F.; Li, S. Azilsartan piperazine salt solvate and monohydrate: Preparation, crystal structure, enhanced solubility and oral bioavailability. *New J. Chem.* **2020**, *44*, 852–860. [[CrossRef](#)]
14. Ning, L.F.; Gong, X.F.; Li, P.; Chen, X.F.; Wang, H.P.; Xu, J. Measurement and correlation of the solubility of estradiol and estradiol-urea co-crystal in fourteen pure solvents at temperatures from 273.15 to 318.15 K. *J. Mol. Liq.* **2020**, *304*, 112599. [[CrossRef](#)]
15. Albert, E.; Andres, P.; Bevill, M.J.; Smit, J.; Nelson, J. Cocrystals of Progesterone. U.S. Patent 20140235595 A1, 6 December 2016.
16. Frišćić, T.; Lancaster, R.W.; Fábíán, L.; Karamertzanis, P.G. Tunable recognition of the steroid  $\alpha$ -face by adjacent  $\pi$ -electron density. *Proc. Natl. Acad. Sci. USA* **2010**, *107*, 13216–13221. [[CrossRef](#)]
17. Zeng, H.; Xiong, J.; Zhao, Z.; Qiao, J.; Wu, X. Preparation of Progesterone co-crystals based on crystal engineering strategies. *Molecules* **2019**, *24*, 3936. [[CrossRef](#)]
18. Samipillai, M.; Rohani, S. The role of higher cofomer stoichiometry ratio in pharmaceutical cocrystals for improving their solid-state properties: The cocrystals of Progesterone and 4-hydroxybenzoic acid. *J. Cryst. Growth* **2019**, *507*, 270–282. [[CrossRef](#)]
19. Bannwarth, C.; Ehlert, S.; Grimme, S. GFN2-xTB-an accurate and broadly parametrized self-consistent tight-binding quantum chemical method with multipole electrostatics and density-dependent dispersion contributions. *J. Chem. Theory Comput.* **2019**, *15*, 1652–1671. [[CrossRef](#)]
20. Pracht, P.; Bohle, F.; Grimme, S. Automated exploration of the low-energy chemical space with fast quantum chemical methods. *Phys. Chem. Chem. Phys.* **2020**, *22*, 7169–7192. [[CrossRef](#)]
21. Grimme, S. Exploration of chemical compound, conformer, and reaction space with meta-dynamics simulations based on tight-binding quantum chemical calculations. *J. Chem. Theory Comput.* **2019**, *15*, 2847–2862. [[CrossRef](#)]
22. Jia, J.L.; Dai, X.L.; Che, H.J.; Li, M.T.; Zhuang, X.M.; Lu, T.B.; Chen, J.M. Cocrystals of regorafenib with dicarboxylic acids: Synthesis, characterization and property evaluation. *Cryst. Eng. Comm.* **2021**, *23*, 653–662. [[CrossRef](#)]

**Disclaimer/Publisher's Note:** The statements, opinions and data contained in all publications are solely those of the individual author(s) and contributor(s) and not of MDPI and/or the editor(s). MDPI and/or the editor(s) disclaim responsibility for any injury to people or property resulting from any ideas, methods, instructions or products referred to in the content.